Hindawi
Mathematical Problems in Engineering
Volume 2022, Article ID 2710285, 13 pages
https://doi.org/10.1155/2022/2710285

Research Article

Brain Tumor Detection using Decision-Based Fusion Empowered with Fuzzy Logic

Aqsa Tahir[1] **Muhammad Asif**[1] **Maaz Bin Ahmad**[2] **Toqeer Mahmood**[3] **Muhammad Adnan Khan**[4,5] **and Mushtaq Ali**[6]

[1]*Department of Computer Science, Lahore Garrison University, Lahore 54000, Pakistan*
[2]*College of Computing and Information Sciences, KIET, Karachi 75190, Pakistan*
[3]*Department of Computer Science, National Textile University, Faisalabad 37610, Pakistan*
[4]*Pattern Recognition and Machine Learning Lab, Department of Software Gachon University, Seongnam 13557, Republic of Korea*
[5]*Riphah School of Computing & Innovation, Faculty of Computing, Riphah International University Lahore Campus, Lahore 54000, Pakistan*
[6]*Department of Computer Science and Information Technology, Hazara University, Mansehra 21300, Pakistan*

Correspondence should be addressed to Toqeer Mahmood; toqeer.mahmood@yahoo.com

Received 25 February 2022; Revised 25 June 2022; Accepted 4 July 2022; Published 21 August 2022

Academic Editor: Muhammad Sajid

Brain tumor is regarded as one of the fatal and dangerous diseases on the planet. It is present in the form of uncontrolled and irregular cells in the brain of an infected individual. Around 60% of glioblastomas turn into large tumors if it is not diagnosed earlier. Some valuable literature is available on tumor diagnosis, but there is room for improvement in overall performance. Machine Learning (ML)-based techniques have been widely used in the medical domain for early diagnostic diseases. The use of ML techniques in conjunction with improved image-guided technology may help in improving the performance of the brain tumor detection process. In this work, an ML-based brain tumor detection technique is presented. Adaptive Back Propagation Neural Network (ABPNN) and Support Vector Machine (SVM) algorithms are used along with fuzzy logic. The fuzzy logic is used to fuse the result of ABPNN and SVM. The proposed technique is developed using the BRATS dataset. Experimental results reveal that the ABPNN model achieved 98.67% accuracy in the training phase and 96.72% accuracy in the testing phase. On the other hand, the SVM model has attained 98.48% and 97.70% accuracy during the training and testing phases. After applying fuzzy logic for decision-based fusion, the overall accuracy of the proposed technique reaches 98.79% and 97.81% for the training and the testing phases, respectively. The comparative analysis with existing techniques shows the supremacy of the proposed technique.

1. Introduction

The term "tumor" refers to a disease that causes swelling or corpus in the body. It can be related to any pathological process. Tumors constitute a significant demonstration of a massive and diverse clutch of ailments known as cancers or usually neoplasms [1]. The brain tumor is one of the fatal and complex types of tumor. It is formed because of a remarkable and aberrant increase in the cells inside the human brain. In ordinary circumstances, the development of a tumor initiates from the blood vessels, cells of the brain, and nerves imminent out of the brain. Over time, the brain tumor has become a significant cause of disabilities and deaths worldwide [2, 3]. Brain tumor location and its capability to feast rapidly make treatment with radiations or surgery alike fighting an opponent hiding amongst caves and minefields. Inappropriately, many safer and easier ways to eliminate a small tumor than a large one are available [4]. About 60% of glioblastomas start as lower small tumors and, over time, become giant tumors.

According to the United States (US), National Cancer Institute estimated new brain tumor cases in the year 2022 are 25,050 (14,170 men and 10,880 women), and estimated deaths caused by brain tumors will be 18,280 [5]. It is also expected that 4,170 children (less than 15 years) will also be affected by a brain tumor. Worldwide, an estimated 308,102 primary brain or spinal cord tumor cases will be reported in 2020. Figure 1 shows the rate of new cases and death rate due to brain tumors in the US.

Figure 2 shows the overall age groupwise number of cases. As it shows, brain tumor cases are high in people aged 60–75. These are moderate in people aged 45–60 and 75–80. Moreover, these are minor in people under 45 and major in people above 80.

In medical science, technology helps scientists examine diseases on a cellular level. It provides antibodies against them in the early stage, which will help to save thousands of lives all-round the globe. Early detection of a brain tumor may help to reduce the casualty rate of brain tumor patients. The brain tumor manual diagnostic procedure is done with the help of domain specialists, which is an extraordinary time taking task. The detection accuracy is highly dependent on the expertise of the domain specialist. Artificial intelligence has brought a revolution in the medical diagnostic domain, improving efficiency and accuracy. The use of ML-based techniques for brain tumor detection may help to speed up the diagnosis process and reduce the death rate. There are some valuable ML-based techniques in the literature for brain tumor detection, but there is room to improve the overall accuracy of these techniques.

This paper presents a brain tumor detection technique in which Adaptive Back Propagation Neural Network (ABPNN) and Support Vector Machine (SVM) algorithms are used along with fuzzy logic. The fuzzy logic is used to fuse the result of ABPNN and SVM, which may help to reduce the false diagnosis. The dataset used in this work to develop the technique is taken from the Kaggle website [7]. It contains Computed tomography (CT) scan details of 3762 patients. It comprises 17 input parameters and one output parameter [7]. The experimental results show that the overall accuracy of the proposed technique is 98.79% and 97.81% for the training and the testing phases, respectively.

The rest of the article is organized as follows. Section 2 presents the literature review in which different methodologies and results are discussed. In Section 3, the proposed methodology is explained. Section 4 describes the experimental results and comparative analysis. Lastly, the paper is concluded in Section 5.

2. Literature Review

Digital image processing and computer vision are playing a vital role in many applications such as remote sensing, autonomous driving, medical image analysis, pose detection, security-based applications, and automated disease detection [8–12]. Recent focus of computer vision community is the use of deep-learning model [13–15] that are computationally expensive. However, at the same time, the research community is still widely presenting machine learning (ML)-based solutions [16–18].

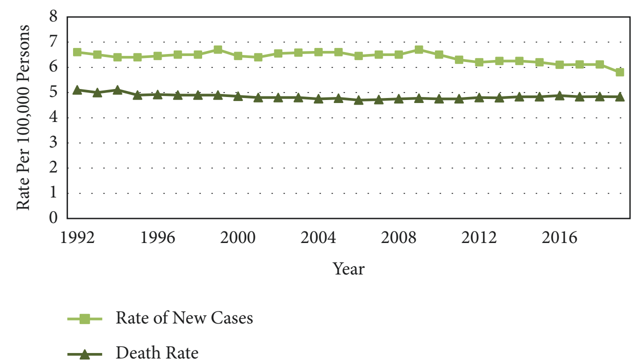

Figure 1: Number of brain tumor cases per year in the US [5].

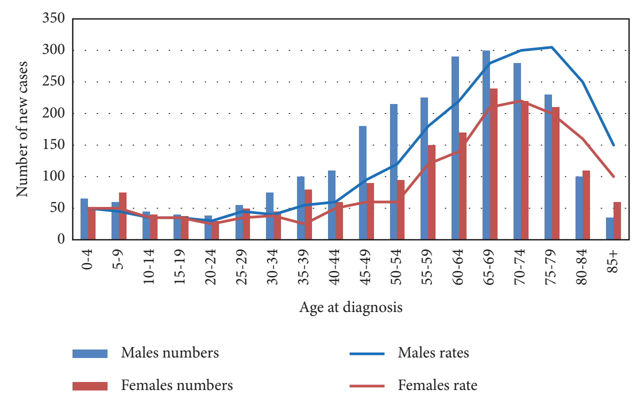

Figure 2: Number of brain tumor cases per age group [6].

In the literature, several attempts have been made to diagnose brain tumors using various ML techniques. Babu et al. [19] have presented a fusion-based brain tumor segmentation technique in which a convolutional neural network (CNN) is used for the fusion of Chan-Vese and level set segmentation methods. They also performed a comparative analysis of fusion-based and clustered-based segmentation techniques to identify the tumor. They claimed that CNN fusion-based segmentation outperforms the clustered-based segmentation technique in terms of segmentation error and minimal loss of information. Abbas et al. [20] have explained Local Independent Projection-based Classification (LIPC) for tumor segmentation using Principal Component Analysis (PCA). Image enhancement and noise removal are done using image preprocessing. To achieve an enhanced and efficient classification score, different textural features are considered and condensed using PCA. The segmentation results demonstrated a 0.95 Dice Score (DS) and 0.72 precision.

Rajan & Sundar [21] have proposed a hybrid-energy-efficient technique for automatic brain tumor segmentation and detection. They used Support Vector Machine (SVM) for brain tumor detection and K-means clustering with Fuzzy C-Means and active contours to perform brain tumor segmentation. They have attained an accuracy of 97.73%. The main limitation of their model is its high computational time because of the numerous techniques involved. Ullah et al. [22] have proposed a brain MRI image classification technique that classifies images into abnormal and normal classes. After performing several preprocessing steps, they used Discrete Wavelet Transform (DWT) for feature extraction. Finally, they used an advanced Deep Neural Network (DNN) to classify whether the brain MRI image is normal or abnormal. They have achieved 95.8% accuracy. Josephine & Murugan [23] have proposed a method for detecting brain cancer utilizing Artificial Neural networks (ANN). They used Gabor features, Gray Level Co-occurrence Matrix (GLCM), and associated texture feature for brain tumor detection. They achieved 96% accuracy on a dataset of 30 MRI images. Ahmmed et al. [24] have proposed a technique for a brain tumor and its stages classification based on SVM and ANN. They used Temper-based K-means and modified Fuzzy C-means (TKFCM) clustering algorithm for segmentation of MRI images. Region property-based features and first-order statistics are extracted from segmented images. The first-order statistic is used to detect tumors from MRI images with the help of SVM. The contrast, the second type of feature helps to detect the stage of the tumor using the ANN. They have achieved an accuracy of 97.37% with a Bit Error Rate (BER) of 0.0294.

Mehmood et al. [6] have proposed a system to assist medical specialists that have the capabilities to perform brain tumor detection, segmentation, and 3D visualization from MRI images. For segmentation, they have used semiautomatic and adaptive threshold selection procedures. To classify a tumor into benign and malignant, the SVM classification model is used. Lastly, the volume marching cube algorithm is used for 3D visualization of the brain and tumors. They have achieved 99% accuracy. Dutta & Bandyopadhyay [25] have proposed a brain tumor detection technique using NGBoost classifier. The authors claimed an accuracy of 98.54%. Dutta & Bandyopadhyay [26] have proposed a technique for brain tumor detection using AdaBoost classifier. They have attained an accuracy of 98.97%. Tahir et al. [27] have proposed a technique for brain tumor detection. They have attained an accuracy of 87%. Munajat & Utaminingrum [28] have presented a GLCM and Back-Propagation Neural Network (BPNN)-based technique for brain tumor detection. They attained an accuracy of 88.03% with an average computation time of 0.601 sec. Ismael & Abdel-Qader [29] have presented a brain tumor detection framework that uses statistical features along with a neural network algorithm. To compute the statistical features, the 2D Gabor filter and 2D DWT are used. The authors claimed 91.9% accuracy for all types of tumors and a specificity of 96% for Meningioma, 96.29% for Glioma, and 96.29% for Pituitary tumors.

Amin et al. [30] have developed an unsupervised clustering method for the segmentation of tumors. A Fused Feature Vector (FFV) is used which is a combination of the Local Binary Pattern (LBP), Gabor Wavelet Features (GWF), segmentation-based fractal texture analysis (SFTA) components, and the histogram of oriented gradients. The classification of tumors among three subtumoral regions is done using Random Forest (RF) classifier. To avoid the overfitting problem, 0.5 holdout cross-validation and five-fold methodologies are applied and detected tumors with reasonable confidence having 100% sensitivity. Ibrahim et al. [31] have developed a neural network-based technique for brain tumor detection through MRI images. It consists of three phases including preprocessing, dimensionality reduction, and classification. The experimental analysis shows that they attained an accuracy of 96.33%. Othman & Basri [32] have designed an automated brain tumor classification technique using PCA and Probabilistic Neural Network (PNN). They used PCA for dimensionality reduction and PNN for classification. The outcomes displayed that the proposed framework accomplished 73% correctness. Najadat et al. [33] have developed a decision tree classifier to recognize anomalies in CT brain pictures. They have achieved an accuracy of 88% on the training set and 58% on 2-fold validation. Balafar et al. [34] have presented a review of brain tumor segmentation techniques. They covered imaging modalities, noise reduction techniques, inhomogeneity correction, magnetic resonance imaging, and segmentation.

Although several valuable studies on brain tumor diagnosis and segmentation using different ML techniques have been proposed, most of these are developed using a limited number of images and have room for improvement in overall performance as explained in Table 1. Therefore, an efficient and accurate technique needs to be developed on a large dataset for diagnosing brain tumors.

3. Proposed Method

This work uses ABPNN and SVM techniques along with fuzzy logic to develop a brain tumor diagnosis system. Figure 3 shows a block diagram of the proposed system. It consists of training and validation phases. The training phase is divided into three layers; data acquisition, preprocessing, and application. In the data acquisition layer, the BRATS dataset is taken from the Kaggle website [7]. It contains Computed Tomography (CT) scan details of 3762 patients. It comprises 17 input parameters and one output parameter that indicates an abnormal or healthy person [7]. Table 2 lists the attributes of the dataset.

In preprocessing layer, data normalization along with missing value handling is performed. Noisy data is dealt with the normalization technique. On the other hand, missing values are resolved using the mean and moving average of the existing values [35]. In the application training layer, two ML algorithms, ABPNN and SVM, are trained using preprocessed data.

The output of ABPNN and SVM is given to the evaluation layer, where miss rate, accuracy, and Mean-Squared Error (MSE) are investigated. Then, an evaluation is done to find whether the Learning Criteria (LC) are met. If LC is met, it passes that data into the cloud. Otherwise, it must be retrained [36].

The next step is to apply fuzzy logic to fuse the results of both techniques to improve the overall performance of the proposed technique. For testing purposes, the extracted attributes from CT scan images of the patient are fed to the fusion-based trained model that predicts whether the patient has a brain tumor or not. When LC is satisfied, the fusion-based trained model is stored on a central server [37].

Table 1: Summary of existing work.

Authors	Techniques	Dataset	Remarks
Babu et al. [19]	CNN fusion followed by Chan-Vese active contour-based segmentation	DS 1-BRATS 2015 and DS 2-brain web	The CNN fusion-based segmentation is better than clustered-based segmentation for brain tumor detection in terms of segmentation error and minimal loss of information
Abbas et al. [20]	PCA and LIPC	MICCAI dataset 30 images	They have performed segmentation with 0.95 DS and 0.72 precision
Rajan & Sundar [21]	SVM, K-means clustering with fuzzy C-means and active contours	41 images	They have attained an accuracy of 97.73%. The main limitation of this model is high computational complexity
Ullah et al. [22]	DWT and DNN	71 images	They have attained an accuracy of 95.8%
Josephine & Murugan [23]	Artificial neural network	30 images	They have achieved 96% accuracy
Ahmmed et al. [24]	TKFCM, SVM, ANN	46 images	They have achieved 97.37% accuracy with 0.0294 BER
Mehmood et al. [6]	SVM and volume marching cube algorithm	256 images	They have achieved 99% accuracy
Dutta & Bandyopadhyay [25]	NGBoost	1644 images	They have attained an accuracy of 98.54%
Dutta & Bandyopadhyay [26]	AdaBoost	1644 images	They have attained an accuracy of 98.97%
Munajat & Utaminingrum [28]	BPNN	3762 images	They have attained an accuracy of 88.03%
Ismael & Abdel-Qader [29]	2D DWT, 2D gabor filter and back-propagation neural network	3064 slices	They have obtained 91.9% accuracy for all types of tumors and a specificity of 96% for meningioma, 96.29% for glioma and 96.29% for pituitary tumors correspondingly
Amin et al. [30]	RF along with GWF HOG, LBP, and SFTA features	531 images	They have claimed 100% sensitivity
Ibrahim et al. [31]	PCA and BPNN	174 images	They have attained 96.33% accuracy
Othman & Basri [32]	PCA and PNN	35 images	They have obtained 73% accuracy
Najadat et al. [33]	Precision tree classifier and ABPNN	25 images	They have achieved 59% accuracy

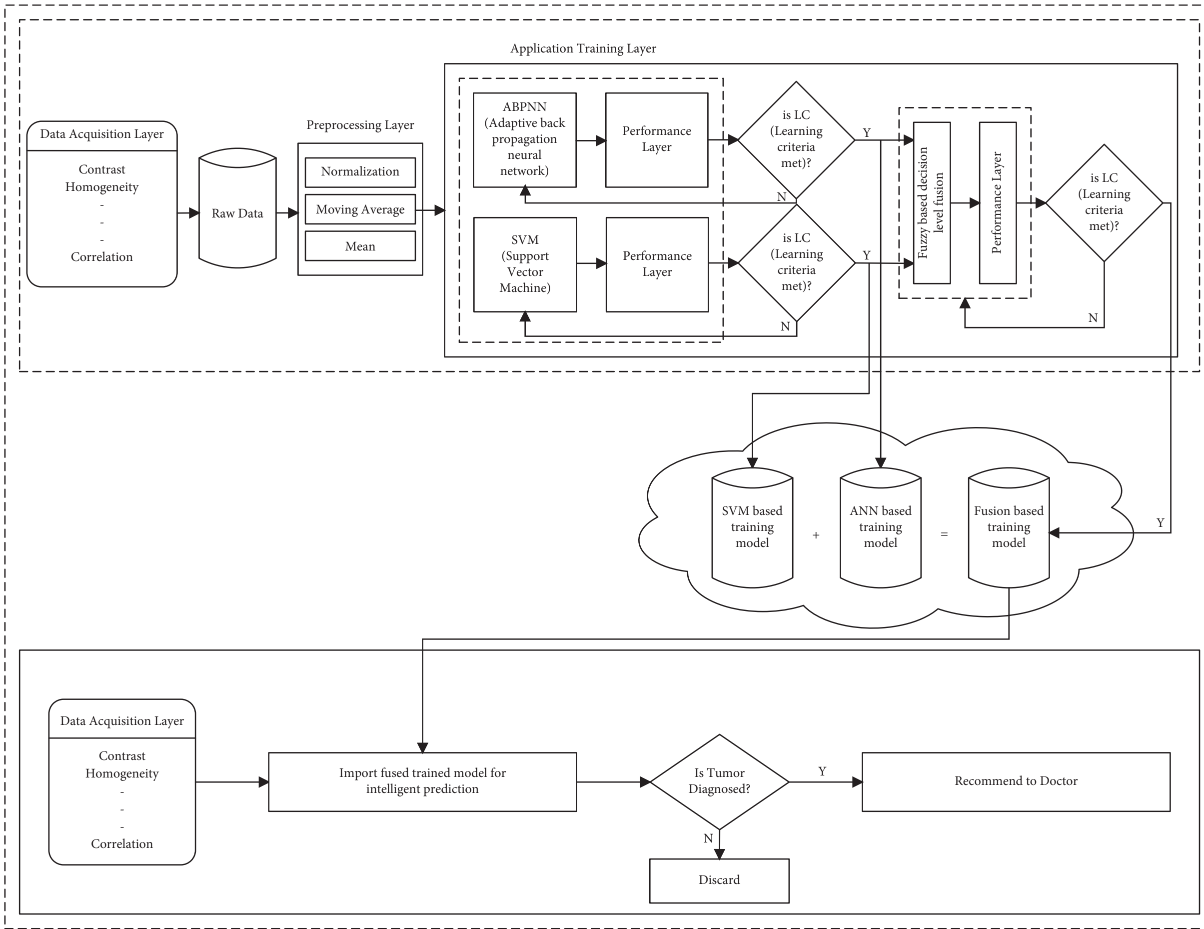

Figure 3: Block diagram of the proposed system.

Table 2: Input and output variables of the proposed DBFEFL system model.

Sr. No	Input/output variable name
Inp-1	Mean
Inp-2	Variance
Inp-3	Standard deviation
Inp-4	Skewness
Inp-5	Kurtosis
Inp-6	Contrast
Inp-7	Energy
Inp-8	(ASM)
Inp-9	Entropy
Inp-10	Homogeneity
Inp-11	Dissimilarity
Inp-12	Correlation
Inp-13	Coarseness
Inp-14	(PSNR)
Inp-15	(SSIM) Index
Inp-16	(MSE)
Inp-17	(DC)
Outp-1	Target (0/1)

3.1. ABPNN. ABPNN consists of the input, output, hidden layers, and the arrangement made from the back-propagation of error and feedforward propagation [38]. In forward propagation, data is composed of the input layer towards the hidden layer, eventually transferred to the output layer. The output layer is then directed in reverse to the procedure of back-propagation error if it is not accepted. Inconsistent weight figures are balanced to limit error and moved towards feedforward [39].

Within the examination of the tumor, the input, output, and hidden layers are being utilized in ABPNN engineering with the feedforward algorithm using bit per data rate and conjunction [40]. In the current algorithm, distinct steps are associated. In the hidden layer, each neuron has an instigation work, e.g., $f(x) = \mathrm{Sigmoid}(x)$. Input capacity for the sigmoid function is presented in equation (1), and the sigmoid function in the hidden layer of the proposed system is composed as presented in equation(2).

$$net_j = \sum_{j=1}^{a}\left(\mu_{ij} * INP_i\right) + \beta_i. \tag{1}$$

$$Out\,p_j = \frac{2}{1 + e^{-net_j}} \tag{2}$$

where $j = 1, 2, 3 \ldots, n$.

The input parameter is taken from the output layer, as shown as follows:

$$€_k = \beta_2 + \sum_{i=1}^{n}\left(\delta_{jk*Out p_j}\right). \quad (3)$$

The activation function of the output layer, as shown as follows:

$$Out p_k = \frac{2}{1+e^{-€_k}} \quad (4)$$

where 1 = 1, 2, 3 . . . , r.

The per output neuron error is calculated with the help of the squared-error function and the sum of each of these to find the total error in (5)

$$\rho = \frac{1}{2}\sum_k \left(\varepsilon_k - Out p_k\right)^2. \quad (5)$$

where the desired output is represented by ε_k and calculated output as $Out p_k$. In (6), the output layer with the rate of weight change is written as

$$\begin{aligned}
&\Delta \mathrm{W} \propto \frac{\partial\rho}{\partial w},\\
&\Delta\delta_{j,k} = -\epsilon\frac{\partial\rho}{\partial\delta_{j,k}},
\end{aligned} \quad (6)$$

$$\begin{aligned}
&\Delta\delta_{j,k} = -\epsilon\frac{\partial\rho}{\partial \mathrm{Outp_k}} * \frac{\partial \mathrm{Outp_k}}{\partial €_k} * \frac{\partial €_k}{\partial\delta_{j,k}},\\
&\Delta\delta_{j,k} = \epsilon\left(\varepsilon_k - \mathrm{Outp}_k\right) * \mathrm{Outp}_k\left(1-\mathrm{Outp}_k\right) * \mathrm{Outp}_j,
\end{aligned} \quad (7)$$

$$\begin{aligned}
&\Delta\delta_{j,k} = \epsilon\,\xi_k \mathrm{Outp}_j,\\
&\xi_k = \left(\varepsilon_k - \mathrm{Outp}_k\right) * \mathrm{Outp}_k\left(1-\mathrm{Outp}_k\right),\\
&\Delta\mu_{ij} \propto -\left[\sum_k \frac{\partial\rho}{\partial \mathrm{Outp}_k} * \frac{\partial \mathrm{Outp}_k}{\partial €_k} * \frac{\partial €_k}{\partial \mathrm{Outp}_j}\right] * \frac{\partial \mathrm{Outp}_j}{\partial \mathrm{net}_j} * \frac{\partial \mathrm{net}_j}{\partial\mu_{ij}},\\
&\Delta\mu_{ij} = -\epsilon\left[\sum_k \frac{\partial\rho}{\partial \mathrm{Outp}_k} * \frac{\partial \mathrm{Outp}_k}{\partial €_k} * \frac{\partial €_k}{\partial \mathrm{Outp}_j}\right] * \frac{\partial \mathrm{Outp}_j}{\partial \mathrm{net}_j} * \frac{\partial \mathrm{net}_j}{\partial\mu_{ij}},\\
&\Delta\mu_{ij} = -\epsilon\left[\sum_k \frac{\partial\rho}{\partial \mathrm{Outp}_k} * \frac{\partial \mathrm{Outp}_k}{\partial €_k} * \frac{\partial €_k}{\partial \mathrm{Outp}_j}\right] * \frac{\partial \mathrm{Outp}_j}{\partial \mathrm{net}_j} * \frac{\partial \mathrm{net}_j}{\partial\mu_{ij}},\\
&\Delta\mu_{ij} = -\epsilon\left[\sum_k \left(\varepsilon_k - \mathrm{Outp}_k\right) * \mathrm{Outp}_k\left(1-\mathrm{Outp}_k\right) * \delta_{j,k}\right] * \mathrm{Outp}_k\left(1-\mathrm{Outp}_k\right) * INP_i,\\
&\Delta\mu_{ij} = -\epsilon\left[\sum_k \left(\varepsilon_k - \mathrm{Outp}_k\right) * \mathrm{Outp}_k\left(1-\mathrm{Outp}_k\right) * \delta_{j,k}\right] * \mathrm{Outp}_j\left(1-\mathrm{Outp}_k\right) * INP_i,\\
&\Delta\mu_{ij} = -\epsilon\left[\sum_k \left(\varepsilon_k - Out p_k\right) * \mathrm{Outp}_k\left(1-\mathrm{Outp}_k\right) * \delta_{j,k}\right] * \mathrm{Outp}_j\left(1-\mathrm{Outp}_k\right) * INP_i,\\
&\xi_j = -\epsilon\left[\sum_k \xi_j\delta_{j,k}\right] * \mathrm{Outp}_j\left(1-\mathrm{Outp}_j\right) * INP_i.
\end{aligned} \quad (8)$$

The value of changed weight will be calculated by switching the values in (7) as intimated in (8), where, Outp_k

$$\Delta\mu_{ij} = \epsilon\,\xi_j INP_i, \quad (9)$$

where

$$\xi_j = \left[\sum_k \xi_j\ \ \delta_{j,k}\right] * \mathrm{Out}p_j\left(1-\mathrm{Out}p_j\right). \quad (10)$$

The hidden and output layers are shown in (11), updating the bias and weight between them.

$$\delta_{j,k}(t+1) = \delta_{j,k}(t) + +\lambda\Delta\delta_{j,k}. \quad (11)$$

The updating values of bias and weight among the input layer and the hidden layer are exhibited as follows:

$$\mu_{ij}(t+1) = \mu_{ij}(t) + +\lambda\Delta\mu_{ij}. \quad (12)$$

The learning rate of the brain tumor system model is represented by "λ."

3.2. SVM. SVM is defined as a supervised ML algorithm that can either be used for regression or classification. Though, it is more commonly used in classification problems. Each data item is plotted in N-dimensional space (N represents total features) per feature's amount of a specific coordinate in the SVM algorithm [41, 42].

As the line equation is

$$\chi_2 = a\chi_1 + b, \tag{13}$$

where "a" is the line slope and "b" is the intercept of the line.

$$a\chi_1 - \chi_2 + b = 0. \tag{14}$$

Let suppose $\overline{x} = (\chi_1, \chi_2)^T$ & $\overline{\omega} = a - 1$. Now the beyond equation could be narrated as

$$\overrightarrow{\omega}.\overline{x} + b = 0. \tag{15}$$

The following equation is the resultant of 2-dimensional vectors. Equation (13) is also referred to as a hyperlane equation. The vector's direction $\overline{x} = (\chi_1, \chi_2)$ is symbolized as $\overline{\omega}$.

$$\omega = \frac{x_1}{\|x\|} + \frac{x_2}{\|x\|}, \tag{16}$$

where

$$\|x\| = \sqrt{x_i^2 + x_2^2 + x_3^2 + \cdots + x_n^2}. \tag{17}$$

As we discern,

$$\begin{aligned}\cos(\sqsupset) &= \frac{x_1}{\|x\|},\\ \cos(\rho) &= \frac{x_2}{\|x\|}.\end{aligned} \tag{18}$$

Equation (16) can be inscribed as

$$\begin{aligned}\omega &= (\cos(\sqsupset), \cos(\rho))\\ \overrightarrow{\omega}\cdot\overrightarrow{x} &= \|\omega\|\|x\|\cos(\sqsupset).\end{aligned} \tag{19}$$

As $\sqsupset = \vartheta - \rho$, then

$$\begin{aligned}\cos(\sqsupset) &= \cos(\vartheta) - \cos(\rho)\\ \cos(\sqsupset) &= \cos(\vartheta)\cos(\rho) - \sin(\vartheta)\sin(\rho).\end{aligned} \tag{20}$$

$\cos(\sqsupset)$ can also be written as

$$\cos(\sqsupset) = \frac{\omega_1}{\|\omega\|}\frac{x_1}{\|x\|} + \frac{\omega_2}{\|\omega\|}\frac{x_2}{\|x\|}. \tag{21}$$

By simplifying the above equation

$$\cos(\sqsupset) = \frac{\omega_1 x_1 + \omega_2 x_2}{\|\omega\|\|x\|}. \tag{22}$$

Put the value of $\cos(\sqsupset)$ is (19)

$$\overrightarrow{\omega}\cdot\overrightarrow{x} = \|\omega\|\|x\|\frac{\omega_1 x_1 + \omega_2 x_2}{\|\omega\|\|x\|}. \tag{23}$$

As the above equation explains the 2-dimensional vectors, for the n-dimensional vector, it can be written as shown in the following equation:

$$\begin{aligned}\overrightarrow{\omega}\cdot\overrightarrow{x} &= \sum_{i=1}^{n}\omega_i x_i\\ &\text{where i} = 1, 2, \ldots, \text{n}.\end{aligned} \tag{24}$$

The above equation is used to validate the correctly classifying the data

$$\text{D} = \ddot{\text{y}}\ (\text{w.x} + \text{b}). \tag{25}$$

"d" is called the functional margin of the dataset and is written as

$$d = \min_{\text{i}=1\ldots m} D_i. \tag{26}$$

The hyperplane is selected as favorable, which has the largest value, where d is called the geometric margin of the dataset and we find out the optimal hyperplane in this article. To find out the optimal hyperplane, use the Lagrangian function, i.e., [43].

$$\begin{aligned}\gamma(\omega, b, \rho) &= \frac{1}{2}\omega\cdot\omega - \sum_{i=1}^{m}\rho_i[y\colon\ (\omega.x + b) - 1],\\ \nabla_\omega\gamma(\omega, b, \rho) &= \omega - \sum_{i=1}^{m}\rho_i y_i x_i = 0\,.\end{aligned} \tag{27}$$

$$\nabla_b\gamma(\omega, b, \rho) = -\sum_{i=1}^{m}\rho_i y_i = 0. \tag{28}$$

Obtaining from (27) and (28), we can write equation (18).

$$\omega = \sum_{i=1}^{m}\rho_i y_i x_i and \sum_{i=1}^{m}\rho_i y_i = 0. \tag{29}$$

By substituting the Lagrangian function ɣ

$$\omega(\rho, b) = \sum_{i=1}^{m}\rho_i - \frac{1}{2}\sum_{i=1}^{m}\cdot\sum_{j=1}^{m}\rho_i\rho_j y_i y_j x_i x_j. \tag{30}$$

Thus, the above equation can also be defined in equation (19).

$$\max_{6}\sum_{i=1}^{m}\rho_i - \frac{1}{2}\sum_{i=1}^{m}\cdot\sum_{j=1}^{m}\rho_i\rho_j y_i y_j x_i x_j. \tag{31}$$

where $i = 1, 2, 3, \ldots, m$.

Because of inequalities in constraints, the "L" multiplier method is spread to the Karush–Kuhn–Tucker (KKT) conditions. KKT complementary condition states that

$$\rho_i[y_i(\omega_i\cdot x^* + b) - 1] = 0. \tag{32}$$

In the above equation, x^* is the optimal point and ϐ is the positive value, and for other points, its values are nearly equal to zero. So, we can write as in equation (20)

$$y_i(\omega_i \cdot x^* + b) - 1 = 0. \quad (33)$$

These are the closest points to the hyperplane, also known as support vectors. According to (33),

$$\omega - \sum_{i=1}^{m} \rho_i y_i x_i = 0. \quad (34)$$

It can also be written as

$$\omega = \sum_{i=1}^{m} \rho_i y_i x_i. \quad (35)$$

Equation (35) gets when we compute the value of b

$$y_i((\omega_i \cdot x^* + b) - 1) = 0. \quad (36)$$

Multiply both sides with y_i

$$y_i^2((\omega_i \cdot x^* + b) - 1) = 0. \quad (37)$$

As we know $y2/i.$ is equal to 1

$$b = y_i - \omega_i \cdot x^*, \quad (38)$$

$$b = \frac{1}{S} \sum_{i=1}^{S} (y_i - \omega.x). \quad (39)$$

In equation (39), S is the number of support vectors, and on the hyperplane, we make the predictions.

The hypothesis function is described in (40)

$$U_{SVM} = \dot{\mathrm{H}}(\omega_i) = \begin{cases} +1 \text{ if } \omega.x + b \geq 0, \\ -1 \text{ if } \omega.x + b < 0. \end{cases} \quad (40)$$

Class +1 will be categorized as an above point in the hyperplane, whereas −1 will be below the hyperplane (congestion not found). So, fundamentally, the main objective of the SVM algorithm is to calculate a hyperplane. It will distinguish the data correctly, and an optimal hyperplane is considered the best [1].

3.3. Decision-Based Fusion Empowered by Fuzzy Logic (DBFEFL). Fusion of data and information can be considered into three levels of abstraction: feature fusion, classifier fusion (also classified as decision-based fusion), and data fusion [44]. Decision fusion is considered a form of data fusion that combines the decisions of multiple classifiers into a mutual decision. It furthermore provides the benefit of recompensing for the insufficiencies of the specific sensor by using one or more than one added sensor [45].

The proposed DBFEFL is all about capability, intelligence, and logic. Fuzzy logic tries to handle problems with an imprecise and open set of data, sorting its chances of getting a flawless result [46]. The proposed DBFEFL for brain tumor diagnosis can be mathematically written as

$$\begin{aligned} &\mu_{ABPNN} \cap \mu_{SVM} (ABPNN, SVM) \\ &\quad = \min[\mu_{ABPNN}(ABPNN), \mu_{SVM}(SVM)] \end{aligned} \quad (41)$$

According to output parameters, ABPNN's possible outcomes can be 0 or 1. Similarly, SVM's possible outcomes can either be 0 or 1. So, according to fuzzy logic, we have four fuzzy rules.

R_1 = If ABPNN outcome is 1 and SVM outcome is 1, a brain tumor is detected.

R_2 = If ABPNN outcome is 0 and SVM outcome is 0, brain tumor is not detected.

R_3 = If ABPNN outcome is 1 and SVM outcome is 0, a brain tumor is detected.

R_4 = If ABPNN outcome is 0 and SVM outcome is 1, a brain tumor is detected.

These rules are shown in the lookup diagram in Figure 4.

Figure 5 describes the surface viewer of the rules, that if ABPNN and SVM are from 0 to 40, the fuzzy decision is 0, which means a brain tumor is not detected. When the value is increased from 40 to 60, fuzzy is between 0-1, which means it can be a tumor. But when the value is greater than 60, the fuzzy decision is 1, which means a brain tumor is detected [47].

Membership function:

$$\begin{aligned} &\text{Detection} = D \\ &(\mu_D(d)) \end{aligned} \left(\mu_{D,\text{No}}(d)\right) = \begin{cases} 1 & 0 \leq d \leq 40, \\ \dfrac{60 - d}{20} & 40 \leq d \leq 60, \\ 0 & 40 \leq d, \end{cases}$$

$$\begin{aligned} &\text{Detection} = D \\ &(\mu_D(d)) \end{aligned} \left(\mu_{D,\text{yes}}(d)\right) = \begin{cases} 0 & d \leq 40, \\ \dfrac{d - 40}{20} & 40 \leq d \leq 60, \\ 1 & 60 \leq d \leq 100. \end{cases} \quad (42)$$

4. Experimental Analysis

The proposed system is developed using MATLAB 2017. For experimental analysis, the dataset is divided into training and testing phases. 2634 samples are used for training, which is 70% of the data sample. 1128 samples are used for testing, i.e., 30% of the data samples [47, 48]. To evaluate the proposed system, several performance measure metrics are used that are computed with the help of equations (27) to (36) [49].

$$\text{Miss rate} = \frac{(O_1/T_0) + (O_0/T_1)}{T_0 + T_1}, \quad (43)$$

$$\text{Accuracy} = \frac{(O_0/T_0) + (O_1/T_1)}{T_0 + T_1}, \quad (44)$$

$$\text{Positive prediction value} = \frac{(O_{10}/T_1)}{(O_0/T_1) + (O_1/T_1)}, \quad (45)$$

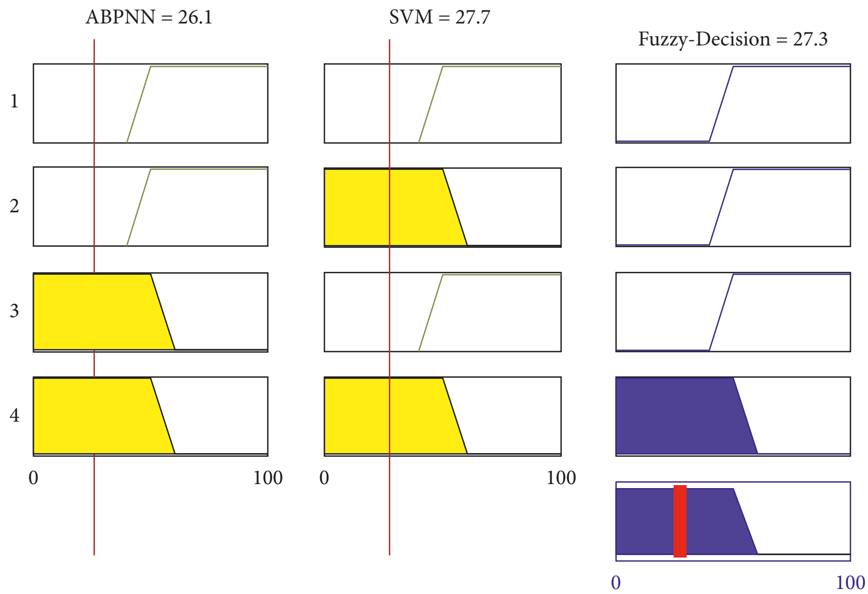

Figure 4: Fuzzy rules lookup diagram.

$$\text{Negative prediction value} = \frac{(O_0/T_0)}{(O_0/T_1) + (O_1/T_1)}, \quad (46)$$

$$\text{Specifcity} = \frac{(O_0/T_0)}{(O_0/T_0) + (O_0/T_1)}, \quad (47)$$

$$\text{Sensitivity} = \frac{(O_1/T_1)}{(O_1/T_0) + (O_1/T_1)}, \quad (48)$$

$$\text{False\_positive\_ratio} = 1 - \text{specificity}, \quad (49)$$

$$\text{False\_positive\_ratio} = 1 - \text{Sensitivity}, \quad (50)$$

$$\text{Likelihood\_ratio\_positive} = \frac{\text{Sensitivity}}{1 - \text{specicity}}, \quad (51)$$

$$\text{Likelihood\_ratio\_negative} = \frac{1 - \text{Sensitivity}}{\text{specifcity}}. \quad (52)$$

The input parameters for the ABPNN and SVM algorithms are listed in Tables 3 and 4, respectively [50–52]. Tables 5 and 6 show the confusion matrix of ABPNN during the training and testing phase, respectively.

Tables 7 and 8 show the confusion matrix of SVM during the training and testing phase, respectively. Tables 9 and 10 show the confusion matrix of DBFEFL during the training and testing phase, respectively.

Table 11 lists the experimental results of the proposed brain tumor detection system at each stage in terms of several performance evaluation metrics [53]. During the testing phase, there is a 97.81% accuracy and a 2.19% miss rate. For the ABPNN model, the accuracy is 98.67% and the miss rate is 1.33% in the training phase. The accuracy and miss rates are 96.72% and 3.28% in the testing phase, respectively. In the SVM model, attained accuracy is 98.48% and the miss rate is 1.52% in the training phase. On the other hand, 97.70% accuracy and 2.3% miss rate are achieved in the testing phase. It can be seen that DBFEFL has an accuracy of 98.79% and a miss rate of 1.21% in the training phase.

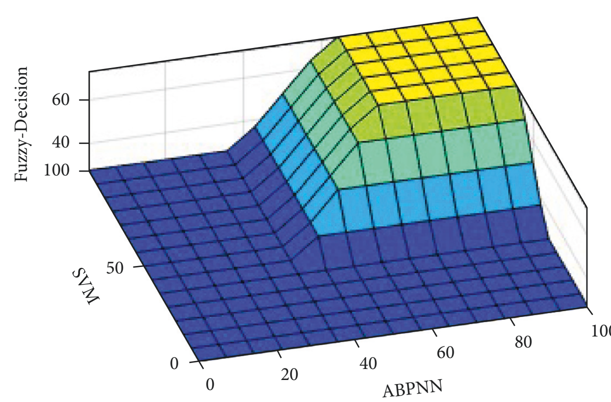

Figure 5: Fuzzy rules surface viewer.

Table 3: Input parameters for ABPNN.

Hyper-parameters	Value
Algorithm	Scaled conjugate gradient
Hidden layers	22
Epochs	11
Momentum	32
Cross-validation	5

Table 4: Input parameters for SVM.

Hyper-parameters	Value
Cross validation	5
Penalty	$L0$, $L1$
Loss	Hinge
Kernel	Linear

Table 5: Confusion matrix of ABPNN (training phase).

	$N = 2634$ (no. of samples)	Result (output) $(\mathbf{O}_0, \mathbf{O}_1)$	
Input	Expected output (T_0, T_1)	O_0 (0)	O_1 (1)
	T_0 = 1682 (0)	1672	10
	T_1 = 952 (1)	25	927

Table 6: Confusion matrix of ABPNN (testing phase).

	$N = 1128$ (no. of samples)	Result (output) $(\mathbf{O}_0, \mathbf{O}_1)$	
Input	Expected output (T_0, T_1)	O_0 (0)	O_1 (1)
	T_0 = 397 (0)	393	4
	T_1 = 731 (1)	33	698

Table 7: Confusion matrix of SVM (training phase).

	$N = 2634$ (no of samples)	Result (output) $(\mathbf{O}_0, \mathbf{O}_1)$	
Input	Expected output (T_0, T_1)	O_0 (0)	O_1 (1)
	T_0 = 1682 (0)	1675	7
	T_1 = 952 (1)	33	919

Table 8: Confusion matrix of SVM (testing phase).

	$N = 1128$ (no of samples)	Result (output) $(\mathbf{O}_0, \mathbf{O}_1)$	
Input	Expected output (T_0, T_1)	O_0 (0)	O_1 (1)
	T_0 = 397 (0)	389	8
	T_1 = 731 (1)	18	713

Table 9: Confusion matrix of DBFEFL (training phase).

	$N = 2634$ (no of samples)	Result (output) $(\mathbf{O}_0, \mathbf{O}_1)$	
Input	Expected output (T_0, T_1)	O_0 (0)	O_1 (1)
	T_0 = 1682 (0)	1675	7
	T_1 = 952 (1)	25	927

Table 10: Confusion matrix of DBFEFL (testing phase).

	$N = 1128$ (no of samples)	Result (output) $(\mathbf{O}_0, \mathbf{O}_1)$	
Input	Expected output (T_0, T_1)	O_0 (0)	O_1 (1)
	T_0 = 397 (0)	390	7
	T_1 = 731 (1)	19	712

Table 11: Experimental results of the proposed system.

Measures	ABPNN (training)	ABPNN (testing)	SVM (training)	SVM (testing)	DBFEFL (training)	DBFEFL (testing)
Accuracy	98.67%	96.72%	98.48%	97.70%	98.79%	97.81%
Miss rate	1.33%	3.28%	1.52%	2.3%	1.21%	2.19%
Sensitivity	98.93%	99.43%	99.24%	98.89%	99.25%	99.03%
Specificity	98.53%	92.25%	98.07%	95.52%	98.53%	95.35%
Precision	97.37%	95.49%	96.54%	97.54%	97.37%	97.4%
Negative predictive value	99.41%	98.99%	99.58%	97.89%	99.58%	98.24%
False positive rate	1.47	7.75	1.93	4.42	1.47	4.65
False negative rate	1.07	0.57	0.76	1.11	0.75	0.97

Table 12 shows a comparative analysis of the proposed system with existing methods using the same dataset taken from the Kaggle website [7]. The experimental results revealed that the proposed method DBFEFL has achieved the highest accuracy with better performance using the latest dataset with the maximum number of samples. The accuracy of the proposed method DBFEFL is 97.81% with the latest dataset of 3762 samples. Whereas the maximum accuracy attained using the Cross-Validated NGBoost Classifier [25] is 98.54%, they use 1644 images. Similarly, the maximum

Table 12: Comparative analysis between the proposed and existing methods.

Author	Technique	BRATS dataset
Proposed	DBFEFL (97.81%)	3672 images
Dutta & Bandyopadhyay [25]	Cross-validated NGBoost classifier (98.54%) Gradient boost (97.37%) AdaBoost (98.18%) Random forest (97.98%) Extra trees (94.13%)	1644 images
Dutta & Bandyopadhyay [26]	Cross-validated AdaBoost classifier (98.97%) Gradient boost (90.69%) Random forest (98.18%) Extra trees (94.33%)	1644 images
Munajat & Utaminingrum [28]	BPNN (87.01%)	3762 images

accuracy attained by using the Cross-Validated AdaBoost Classifier [26] is 98.97%, but similarly, they are using 1644 images. The accuracy using BPNN [28] is 87.01% using the same number of samples.

5. Conclusion

Early detection of brain tumors helps to decrease the casualty rate of brain tumor patients. The brain tumor manual diagnostic procedure is done with the help of domain specialists, which is an extraordinary time taking task. To automate this process, this paper presented a system for brain tumor detection that exploited ABPNN, SVM, and fuzzy logic to achieve the desired results. The outcomes of ABPNN and SVM are fused using fuzzy logic to increase the system's overall accuracy. The experimental results showed an accuracy of 98.30% and a miss rate of 1.7%. This research will be helpful in the medical science field. It can be deployed in OPD for brain tumor detection. It can be transformed into an interactive app that will take CT-scan images as an input parameter and categorize the patient as infected or normal. It may be helpful for doctors as an assistant hand for them that may strengthen their opinion regarding the diagnosis of the brain tumor patient.

Data Availability

The data used to support the study's findings are available from the corresponding author upon request.

Conflicts of Interest

The authors declare that they have no conflicts of interest.

References

[1] P. Tanwar, V. Jain, C.-M. Liu, and V. Goyal, *Big Data Analytics and Intelligence: A Perspective for Health Care*, Emerald Publishing Limited, West Yorkshire, England, 2020.

[2] P. Jegannathan, "Brain tumor detection using convolutional neural network," *Turkish Journal of Computer and Mathematics Education (TURCOMAT)*, vol. 12, pp. 686–692, 2021.

[3] M. Masood, T. Nazir, M. Nawaz et al., "A novel deep learning method for recognition and classification of brain tumors from MRI images," *Diagnostics*, vol. 11, no. 5, p. 744, 2021.

[4] D. Febrianto, I. Soesanti, and H. Nugroho, "Convolutional neural network for brain tumor detection," *IOP Conference Series: Materials Science and Engineering*, vol. 771, no. (1), Article ID 012031, 2020.

[5] A. Noone, N. Howlader, M. Krapcho, D. Miller, A. Brest, and M. Yu, "Cancer stat facts: brain and other nervous system cancer," *SEER cancer statistics review*, vol. 2015, 1975, https://seer.cancer.gov/statfacts/html/childbrain.html.

[6] I. Mehmood, M. Sajjad, K. Muhammad et al., "An efficient computerized decision support system for the analysis and 3D visualization of brain tumor," *Multimedia Tools and Applications*, vol. 78, no. 10, pp. 12723–12748, 2019.

[7] J. Bohaju, "Brain tumor," 2020, https://www.kaggle.com/dsv/1370629.

[8] Q. Zou, K. Xiong, Q. Fang, and B. Jiang, "Deep imitation reinforcement learning for self-driving by vision," *CAAI Transactions on Intelligence Technology*, vol. 6, no. 4, pp. 493–503, 2021.

[9] J. Zhang, G. Ye, Z. Tu et al., "A spatial attentive and temporal dilated (SATD) GCN for skeleton-based action recognition," *CAAI Transactions on Intelligence Technology*, vol. 7, no. 1, pp. 46–55, 2022.

[10] A. Shabbir, A. Rasheed, H. Shehraz et al., "Detection of glaucoma using retinal fundus images: a comprehensive review," *Mathematical Biosciences and Engineering*, vol. 18, no. 3, pp. 2033–2076, 2021.

[11] A. Shabbir, N. Ali, J. Ahmed et al., "Satellite and scene image classification based on transfer learning and fine tuning of ResNet50," *Mathematical Problems in Engineering*, vol. 2021, pp. 2021–2118.

[12] A. Rehman, N. Abbas, T. Saba, T. Mahmood, and H. Kolivand, "Rouleaux red blood cells splitting in microscopic thin blood smear images via local maxima, circles drawing, and mapping with original RBCs," *Microscopy Research and Technique*, vol. 81, no. 7, pp. 737–744, 2018.

[13] S. Fatima, N. A. Aslam, I. Tariq, and N. Ali, "Home security and automation based on internet of things: a comprehensive review," *IOP Conference Series: Materials Science and Engineering*, vol. 899, no. (1), Article ID 012011, 2020.

[14] X. Zhang and G. Wang, "Stud pose detection based on photometric stereo and lightweight YOLOv4," *Journal of Artificial Intelligence and Technology*, vol. 2, pp. 32–37, 2022.

[15] M. Asif, M. Bin Ahmad, S. Mushtaq, K. Masood, T. Mahmood, and A. Ali Nagra, "Long multi-digit number recognition from images empowered by deep convolutional neural networks," *The Computer Journal*, 2021.

[16] M. Tahir, I. A. Taj, P. A. Assuncao, and M. Asif, "Fast video encoding based on random forests," *Journal of Real-Time Image Processing*, vol. 17, no. 4, pp. 1029–1049, 2020.

[17] M. Asif, A. A. Nagra, M. B. Ahmad, and K. Masood, "Feature selection empowered by self-inertia weight adaptive particle swarm optimization for text classification," *Applied Artificial Intelligence*, vol. 36, no. 1, Article ID 2004345, 2022.

[18] R. Ashraf, K. B. Bajwa, and T. Mahmood, "Content-based image retrieval by exploring bandletized regions through support vector machines," *Journal of Information Science and Engineering*, vol. 32, pp. 245–269, 2016.

[19] K. R. Babu, P. Nagajaneyulu, and K. S. Prasad, "Performance analysis of CNN fusion based brain tumour detection using Chan-Vese and level set segmentation algorithms," *International Journal of Signal and Imaging Systems Engineering*, vol. 12, no. 1/2, p. 62, 2020.

[20] K. Abbas, P. W. Khan, K. T. Ahmed, and W.-C. Song, "Automatic brain tumor detection in medical imaging using machine learning," in *Proceedings of the 2019 International Conference on Information and Communication Technology Convergence*, pp. 531–536, Jeju, Korea (South), October2019.

[21] P. G. Rajan and C. Sundar, "Brain tumor detection and segmentation by intensity adjustment," *Journal of Medical Systems*, vol. 43, no. 8, p. 282, 2019.

[22] Z. Ullah, M. U. Farooq, S.-H. Lee, and D. An, "A hybrid image enhancement based brain MRI images classification technique," *Medical Hypotheses*, vol. 143, Article ID 109922, 2020.

[23] S. Josephine and S. Murugan, "Brain tumor grade detection by using ANN," *International Journal of Engineering and Advanced Technology*, vol. 8, no. 6, pp. 4175–4178, 2019.

[24] R. Ahmmed, A. S. Swakshar, M. F. Hossain, and M. A. Rafiq, "Classification of tumors and it stages in brain MRI using support vector machine and artificial neural network," in *Proceedings of the 2017 International Conference on Electrical, Computer and Communication Engineering*, pp. 229–234, Cox's Bazar, Bangladesh, Feb2017.

[25] S. Dutta and S. K. Bandyopadhyay, "Revealing brain tumor using cross-validated NGBoost classifier," *International Journal of Machine Learning and Networked Collaborative Engineering*, vol. 4, no. 1, pp. 12–20, 2020.

[26] S. Dutta and S. Bandyopadhyay, "Cross-validated AdaBoost classifier used for brain tumor detection," *EC Neurology*, vol. 12, pp. 50–57, 2020.

[27] B. Tahir, S. Iqbal, M. Usman Ghani Khan et al., "Feature enhancement framework for brain tumor segmentation and classification," *Microscopy Research and Technique*, vol. 82, no. 6, pp. 803–811, 2019.

[28] A. R. Munajat and F. Utaminingrum, "Brain tumor detection system based on sending email using Gray level Co-occurrence matrix and back-propagation neural network," in *Proceedings of the 6th International Conference on Sustainable Information Engineering and Technology*, vol. 2021, pp. 321–326, 2021.

[29] M. R. Ismael and I. Abdel-Qader, "Brain Tumor Classification via Statistical Features and Back-Propagation Neural Network," in *Procedings of the 2018 IEEE international conference on electro/information technology (EIT)*, pp. 0252–0257, Rochester, MI, USA, Oct2018.

[30] J. Amin, M. Sharif, M. Raza, and M. Yasmin, "Detection of brain tumor based on features fusion and machine learning," *Journal of Ambient Intelligence and Humanized Computing*, pp. 1–17, 2018.

[31] W. H. Ibrahim, A. A. A. Osman, and Y. I. Mohamed, "MRI brain image classification using neural networks," in *Proceedings of the 2013 International Conference on Computing, Electrical and Electronic Engineering*, pp. 253–258, Khartoum Sudan, Augest2013.

[32] M. F. Othman and M. A. M. Basri, "Probabilistic neural network for brain tumor classification," in *Proceedings of the 2011 Second International Conference on Intelligent Systems, Modelling and Simulation*, pp. 136–138, Phnom Penh, Cambodia, January2011.

[33] H. Najadat, Y. Jaffal, O. Darwish, and N. Yasser, "A classifier to detect abnormality in CT brain images," in *Proceedings of the The 2011 IAENG International Conference on Data Mining and Applications*, pp. 374–377, 2011.

[34] M. A. Balafar, A. R. Ramli, M. I. Saripan, and S. Mashohor, "Review of brain MRI image segmentation methods," *Artificial Intelligence Review*, vol. 33, no. 3, pp. 261–274, 2010.

[35] P. Ambily, S. P. James, and R. R. Mohan, "Brain tumor detection using image fusion and neural network," *International Journal of Engineering Research and General Science*, vol. 3, pp. 1383–1388, 2015.

[36] A. Ata, M. A. Khan, S. Abbas, M. S. Khan, and G. Ahmad, "Adaptive IoT empowered smart road traffic congestion control system using supervised machine learning algorithm," *The Computer Journal*, vol. 64, no. 11, pp. 1672–1679, 2021.

[37] T. Ali, K. Masood, M. Irfan et al., "Multistage segmentation of prostate cancer tissues using sample entropy texture analysis," *Entropy*, vol. 22, no. 12, p. 1370, 2020.

[38] V. S. Selvam and S. Shenbagadevi, "Brain tumor detection using scalp EEG with modified wavelet-ICA and multi layer feed forward neural network," in *Proceedings of the 2011 Annual International Conference of the IEEE Engineering in Medicine and Biology Society*, pp. 6104–6109, MA, USA, Augest2011.

[39] C. Megha and J. Sushma, "Detection of brain tumor using machine learning approach," in *Proceedings of the International Conference on Advances in Computing and Data Sciences*, pp. 188–196, Ghaziabad, India, April2019.

[40] J. S. Paul, A. J. Plassard, B. A. Landman, and D. Fabbri, "Deep learning for brain tumor classification," *Medical Imaging 2017: Biomedical Applications in Molecular, Structural, and Functional Imaging*, vol. 10137, pp. 253–268, 2017.

[41] R. M. Adnan, X. Yuan, O. Kisi, and Y. Yuan, "Streamflow forecasting using artificial neural network and support vector machine models," *American Academic Scientific Research Journal for Engineering, Technology, and Sciences*, vol. 29, pp. 286–294, 2017.

[42] M. Alyas Khan, M. Ali, M. Shah et al., "Machine learning-based detection and classification of walnut fungi diseases," *Intelligent Automation & Soft Computing*, vol. 30, no. 3, pp. 771–785, 2021.

[43] N. Abdullah, U. K. Ngah, and S. A. Aziz, "Image classification of brain MRI using support vector machine," in *Proceedings of the 2011 IEEE International Conference on Imaging Systems and Techniques*, pp. 242–247, Batu Ferringhi, Malaysia, May2011.

[44] P. R. Kshirsagar, A. N. Rakhonde, and P. Chippalkatti, "MRI image based brain tumor detection using machine learning," *Test Engineering and Management*, vol. 81, pp. 3672–3680, 2020.

[45] J. Amin, M. Sharif, A. Haldorai, M. Yasmin, and R. S. Nayak, *Brain Tumor Detection and Classification Using Machine Learning: A Comprehensive Survey*, pp. 1–23, Complex & Intelligent Systems, Saudi Arabia, 2021.

[46] G. Ramkumar, R. Thandaiah Prabu, N. Phalguni Singh, and U. Maheswaran, "Experimental analysis of brain tumor

detection system using Machine learning approach," *Materials Today Proceedings*, 2021.

[47] A. Keerthana, B. Kavin Kumar, K. Akshaya, and S. Kamalraj, "Brain tumour detection using machine learning algorithm," *Journal of Physics: Conference Series*, vol. 1937, no. 1, Article ID 012008, 2021.

[48] G. Manogaran, P. M. Shakeel, A. S. Hassanein, P. Malarvizhi Kumar, and G. Chandra Babu, "Machine learning approach-based gamma distribution for brain tumor detection and data sample imbalance analysis," *IEEE Access*, vol. 7, pp. 12–19, 2019.

[49] J. Amin, M. Sharif, M. Raza, T. Saba, and M. A. Anjum, "Brain tumor detection using statistical and machine learning method," *Computer Methods and Programs in Biomedicine*, vol. 177, pp. 69–79, 2019.

[50] S. H. Javed, M. B. Ahmad, M. Asif, S. H. Almotiri, K. Masood, and M. A. A. Ghamdi, "An intelligent system to detect advanced persistent threats in industrial internet of things (I-IoT)," *Electronics*, vol. 11, no. 5, p. 742, 2022.

[51] A. Hussain, M. Asif, M. B. Ahmad, T. Mahmood, and M. A. Raza, "Malware detection using machine learning algorithms for windows platform," in *Proceedings of International Conference on Information Technology and Applications*, pp. 619–632, Mragowo, Poland, Oct2022.

[52] D. Jude Hemanth and J. Anitha, "Modified genetic algorithm approaches for classification of abnormal magnetic resonance brain tumour images," *Applied Soft Computing*, vol. 75, pp. 21–28, 2019.

[53] K. Sharma, A. Kaur, and S. Gujral, "Brain tumor detection based on machine learning algorithms," *International Journal of Computer Application*, vol. 103, no. 1, pp. 7–11, 2014.